



**HAL**  
open science

# Disentangling the complex network of non-covalent interactions in fenchone hydrates via rotational spectroscopy and quantum chemistry

Mhamad Chrayteh, Ecaterina Burevschi, Donatella Loru, Thérèse R Huet, Pascal Dréan, M. Eugenia Sanz

## ► To cite this version:

Mhamad Chrayteh, Ecaterina Burevschi, Donatella Loru, Thérèse R Huet, Pascal Dréan, et al.. Disentangling the complex network of non-covalent interactions in fenchone hydrates via rotational spectroscopy and quantum chemistry. *Physical Chemistry Chemical Physics*, 2021, 23 (36), pp.20686-20694. 10.1039/d1cp02995a . hal-04219895

**HAL Id: hal-04219895**

**<https://hal.science/hal-04219895>**

Submitted on 27 Sep 2023

**HAL** is a multi-disciplinary open access archive for the deposit and dissemination of scientific research documents, whether they are published or not. The documents may come from teaching and research institutions in France or abroad, or from public or private research centers.

L'archive ouverte pluridisciplinaire **HAL**, est destinée au dépôt et à la diffusion de documents scientifiques de niveau recherche, publiés ou non, émanant des établissements d'enseignement et de recherche français ou étrangers, des laboratoires publics ou privés.

Cite this: DOI: 00.0000/xxxxxxxxxx

# Disentangling the complex network of non-covalent interactions in fenchone hydrates via rotational spectroscopy and quantum chemistry<sup>†</sup>

Mhamad Chrayteh,<sup>a</sup> Ecaterina Burevski,<sup>b</sup> Donatella Loru,<sup>b,‡</sup> Thérèse R. Huet,<sup>a</sup> Pascal Dréan<sup>a\*</sup> and Maria Eugenia Sanz<sup>b</sup>

Received Date  
Accepted Date

DOI: 00.0000/xxxxxxxxxx

The hydrates of the monoterpene fenchone ( $C_{10}H_{16}O$ ) $\cdot(H_2O)_n$  ( $n = 1, 2, 3$ ) were investigated both by computational chemistry and microwave spectroscopy. Two monohydrates, three dihydrates and for the first time three trihydrates have been identified through the observation of the parent and  $^{18}O$  isotopologues in the rotational spectrum from 2 to 20 GHz. For each hydrate, the sets of rotational constants enabled the determination of the substitution coordinates of the oxygen water atoms as well as an effective structure accounting for the arrangement of the water molecules around fenchone. The hydrates consist in water chains anchored to fenchone by a  $-C=O\cdots H-O$  hydrogen bond and further stabilized by numerous  $-H-O\cdots H-C-$  dispersive secondary interactions with the alkyl hydrogen atoms of fenchone.

## 1 Introduction

The voluptuous and pleasant smells of some plants and fruits are due to volatile organic compounds present in their essential oils. The sweet atmosphere produced by citrus trees on a warm summer evening is due to limonene. The strong smell of pine trees comes from pinenes. These molecules are olefins comprising 10 atoms of carbon and are part of a class of molecules called monoterpenes. Their oxygenated derivatives - alcohols, aldehydes and ketones - are called monoterpenoids and they also exhibit pleasant or strong smells. For instance, the delicate odor of lavender is due to linalool, the rather strong odor of rosemary comes from verbenone. The previous considerations should not hide the fact that these compounds are also atmospheric pollutants involved in the formation of atmospheric secondary organic aerosols (SOAs) and ozone in a complex interplay with oxidants typical of human activities, like the nitrogen oxides  $NO_x$ .<sup>1,2</sup> The formation of SOAs is a major environmental problem, influencing air quality and global climate change.<sup>3,4</sup> Although the mechanisms of SOAs formation are far from being fully elucidated,<sup>5,6</sup> it is believed that water participates, modifying reaction rates and

the composition of final products.<sup>7–11</sup> Some recent theoretical studies aimed at taking into account the microsolvation of reactants in chemical mechanisms,<sup>12</sup> or to develop efficient models to predict the geometry of microsolvated species and to approach solvation.<sup>13–15</sup> The study of the interaction of water with the precursors of SOAs is then of crucial importance to benchmark these novel approaches.

Rotational spectroscopy has been used for decades to study molecular complexes,<sup>16</sup> first limited to small size complexes, but evolving towards complexes of larger and larger sizes as the access to high quality computational chemistry improved along with the development of supersonic expansions coupled to chirped-pulse Fourier transform microwave spectrometers (FTMW). Once formed, the molecular clusters are frozen in the expansion and stabilized by the absence of collisions, allowing their detection. Rotational spectroscopy is particularly well suited to identify how water molecules are attached to a substrate since the technique is very sensitive to any change in the geometry of a molecular species. It is particularly useful to distinguish molecular clusters with extremely close geometries. It was successfully applied to the study of the microhydration of several monoterpenoids and monoterpenes including camphor,<sup>17</sup> verbenone,<sup>18</sup> myrtenal and perillaldehyde,<sup>19,20</sup> verbenol,<sup>21</sup> and limonene.<sup>22</sup> These studies have provided novel information on the interactions of terpenoids with one to three water molecules. In all of them, the first water molecule binds to the nucleophile in the terpenoid, either a carbonyl or hydroxyl oxygen, by establishing a  $O-H\cdots O$  hydrogen bond (HB). Additional water molecules bind to the first water and the whole ensemble is further stabilised by secondary inter-

<sup>a</sup> University of Lille, CNRS, UMR 8523 - PhLAM - Physique des Lasers, Atomes et Molécules, F-59000 Lille, France. Fax: +33 (0)3 20 33 70 20; Tel: +33 (0)3 20 43 49 05; E-mail: pascal.drean@univ-lille.fr

<sup>b</sup> Department of Chemistry, King's College London, London, SE1 1DB, United Kingdom.

<sup>†</sup> Electronic Supplementary Information (ESI) available: [Tables of measured lines, Tables of spectroscopic constants of  $^{18}O$  isotopic species, Tables of experimental structural parameters. See doi]

<sup>‡</sup> Present address : Deutsches Elektronen-Synchrotron (DESY), Notkestraße 85, D-22607 Hamburg.

actions between the water oxygen atoms and the alkyl hydrogens of the terpenoid.

Here we report on the hydrates of fenchone, a terpenoid that is an isomer of camphor. Fenchone shares the same bicyclic structure as camphor, but differs in the position of two of the three methyl groups attached to the bicyclic skeleton. The rotational spectrum of fenchone has been investigated by Loru *et al.*,<sup>23</sup> as well as its complexes with ethanol,<sup>24</sup> and with phenol and benzene.<sup>25</sup> We have studied fenchone-water complexes using a chirped-pulse microwave spectrometer at King's College London which allows to have a global view of the rotational spectrum in the 2-8 GHz range, and a cavity-based spectrometer in Lille allowing measurements up to 20 GHz with an accuracy of up to 1 kHz. Our investigation has resulted in the experimental characterisation of two monohydrates, three dihydrates and for the first time of three trihydrates, and has revealed a complex network of non-covalent interactions determining their preferred configurations.

## 2 Methods

Computational chemistry with the Gaussian 16 suite of programs<sup>26</sup> was used to optimize feasible geometries of the hydrates, from which the equilibrium rotational constants, the permanent dipole moments and the energy ordering of the various conformers were obtained. The CREST program<sup>27,28</sup> was used in order to exhaustively map the conformations the hydrates adopt. Calculations were carried out at two levels of theory which proved their reliability in previous studies. The density functional B3LYP<sup>29</sup> with Grimme's dispersion scheme<sup>30-32</sup> and Becke-Johnson's dumping functions<sup>33-36</sup> was used in combination with the Ahlrichs def2-TZVP basis set.<sup>37</sup> *Ab initio* calculations were performed at the Møller-Plesset second order of theory<sup>38</sup> with the 6-311++G(d,p) basis set.<sup>39-41</sup> Harmonic frequencies calculations were carried out at the optimized geometries to confirm that the geometries corresponded to true minima and to obtain the zero-point energy (ZPE) corrections. The basis sets superposition errors (BSSE) were calculated at the *ab initio* optimized geometries using the Boys-Bernardi<sup>42</sup> counterpoise method in order to obtain the interaction energy between water and fenchone, which was independently decomposed into individual Coulombic, exchange, induction, and dispersive contributions using the symmetry-adapted perturbation theory (SAPT2+)<sup>43,44</sup> in combination with the aug-cc-PVDZ basis set. SAPT calculations were performed considering two fragments: the host molecule fenchone and either one water molecule, the water dimer or the water trimer. This may be a rough approximation for the complexes of fenchone with two and three water molecules but it provides insight on the different energy contributions. Non-covalent interactions (NCI) analysis<sup>45,46</sup> is a tool to visualize the interactions as isosurfaces ( $s = 0.5$ ) with a color scale indicating the strengths of attractive (blue) or repulsive (red) interactions using the VMD program.<sup>47</sup>

Chirped-pulse (CP) and cavity-based microwave Fourier transform spectrometers in respectively London and Lille were used in the experimental study of the hydrates. In both experiments, R-fenchone (Sigma-Aldrich,  $\geq 98\%$ ) was placed in a bespoke heating nozzle inside the vacuum chamber in London and outside in

Lille,<sup>48</sup> at a temperature of ca. 373 K. Water was added to the injection line in a reservoir outside the chamber at room temperature. Fenchone and water were seeded in neon at 5 bar and conducted to the vacuum chamber. The fenchone-water complexes are produced by collisions in the initial stages of the supersonic expansion. The CP-FTMW spectrometer at King's College London<sup>23,49</sup>, which operates in the 2-8 GHz frequency range, was used to record the broadband microwave spectrum of fenchone-water. The molecular species present in the supersonic expansion were polarized by four chirped microwave pulses of  $4\mu\text{s}$  duration. Each microwave pulse was followed by the collection of the molecular free induction decay (FID) for  $20\mu\text{s}$  and transformed to the frequency domain using a FFT algorithm. The final rotational spectrum of fenchone-water recorded had 1.1M FIDs. In Lille, we have employed a cavity-based spectrometer working in the frequency range 2 - 20 GHz. The orifice was opened during  $800\mu\text{s}$  at a repetition rate of 1 Hz and the species were polarized by a  $2\mu\text{s}$  microwave pulse. A heterodyne detection lowering the frequency of the FIDs down to 30 MHz. They were digitized using an acquisition device operating at 120 MHz. After the Fourier transform, lines were observed as Doppler doublet due to the coaxial arrangement of the cavity mirrors and of the jet. The frequency of the transitions was taken as the arithmetic average of the frequencies of each component of the doublet. According to the number of acquired samples, an accuracy of 1 to 2 kHz was expected. In order to study the complexes containing the  $^{18}\text{O}$  water isotopologues, a 1:1 mixture of  $\text{H}_2^{16}\text{O}$  and  $\text{H}_2^{18}\text{O}$  (97% purity, Chem-Cruz) was used in London, while in Lille we used a sample of  $\text{H}_2^{18}\text{O}$  (98% purity, Sigma-Aldrich or Eurisotop) without dilution with normal water. The final CP spectrum of fenchone with isotopically  $^{18}\text{O}$  enriched water was 6.8M FIDs.

## 3 Results and discussion

A systematic search of the possible conformers was first carried out using the conformer-rotamer ensemble sampling (CREST) tool program.<sup>27,28,50</sup> The geometries of the lowest energy conformers (two monohydrates, four dihydrates and five trihydrates in an energy window of  $8\text{kJ mol}^{-1}$ ) were further optimized by DFT and *ab initio* calculations, which provide an estimate of the equilibrium rotational constants, of the permanent dipole moment components along the three principal inertial axis, and of the relative energies between conformers. The hydrates are named according to the number of their water molecules (1w, 2w, or 3w), followed by a roman numeral indicating their relative stability, starting at I for the lowest energy conformers. The results of the calculations are summarized in Table 1.

According to the MP2 calculated permanent dipole moment components, the rotational spectrum of the hydrates should be composed of rather intense *a*-type transitions with much weaker *b*- and *c*-type transitions. The  ${}^aR_{01}$  (corresponding to selections rules  $\Delta J = +1$ ,  $\Delta K_a = 0$  and  $\Delta K_c = +1$ ) groups of transitions of a given species form clusters of lines regularly spaced by the sum of the rotational constants  $B + C$ , rather distinctly visible in a broadband spectrum. The two intense transitions  $J_{0,J} \leftarrow (J-1)_{0,(J-1)}$  and  $J_{1,J} \leftarrow (J-1)_{1,(J-1)}$   ${}^aR_{0,1}$  are predicted to be close and can also be used as starting point in the identification, as shown in

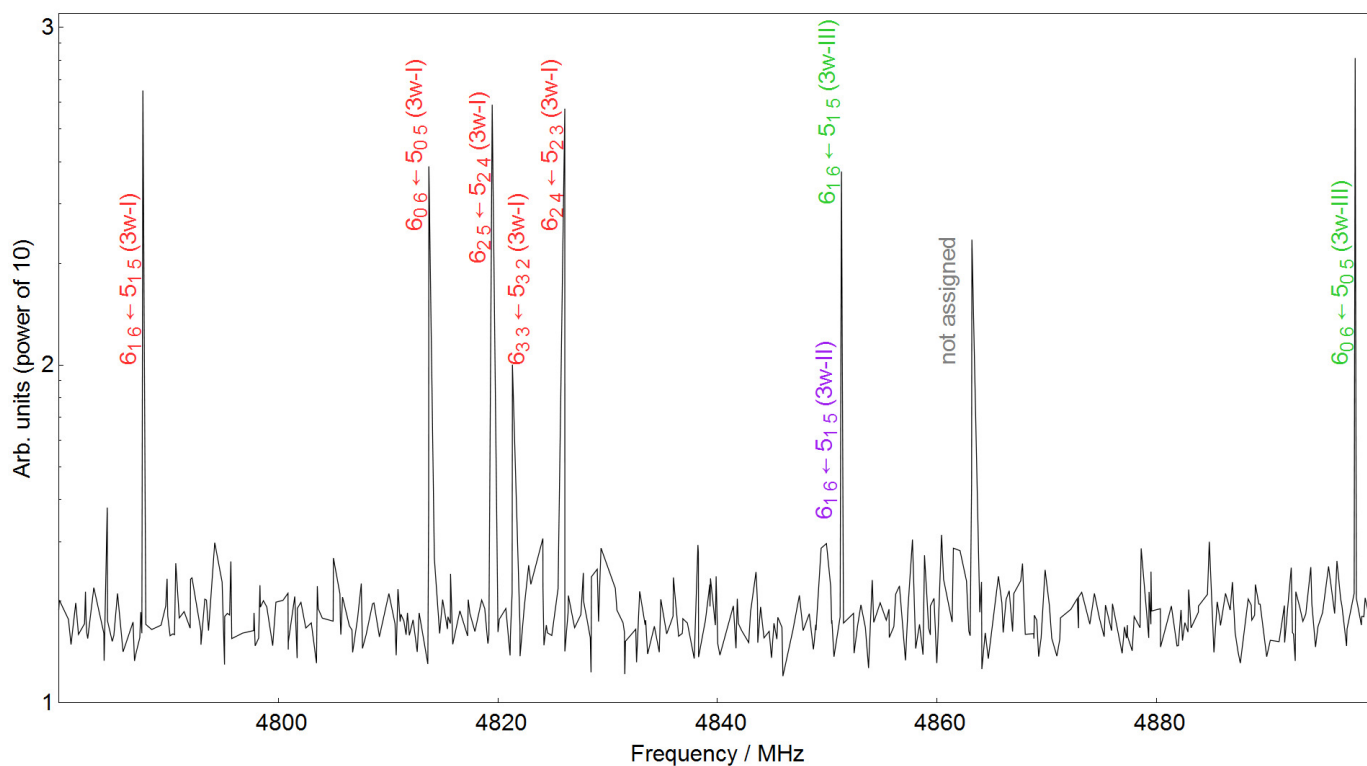


**Fig. 1** A portion of the fenchone-water spectrum, showing peaks of three different trihydrates, using the cavity-based spectrometer in Lille. Repetition rate of the nozzle : 1 Hz, number of averaged FIDs per step : 30, pulse condition set for a dipole moment of  $\approx 1.5$ D. Note in particular the two close intense transitions  $6_{16} \leftarrow 5_{15}$  and  $6_{06} \leftarrow 5_{05}$  of 3w-I and 3w-III that can serve as starting points for assignment. The fact that the  $6_{16} \leftarrow 5_{15}$  transition of 3w-II is weak is due to the fact that the line was on the side of the cavity mode during the automatic survey.

**Table 1** Computed rotational constants, dipole moments and relative energies of the hydrates of fenchone

|        | MP2/6-311++G(d,p)  |                             |              | B3LYP-D3BJ/def2-TZVP |                             |              |
|--------|--------------------|-----------------------------|--------------|----------------------|-----------------------------|--------------|
|        | $A/B/C^a$          | $ \mu_a / \mu_b / \mu_c ^b$ | $\Delta E^c$ | $A/B/C^a$            | $ \mu_a / \mu_b / \mu_c ^b$ | $\Delta E^c$ |
| 1w-I   | 1297.6/746.8/614.1 | 2.9/0.3/0.2                 | 0.0          | 1301.8/754.8/620.6   | 3.0/0.4/0.3                 | 0.0          |
| 1w-II  | 1163.7/796.2/675.1 | 2.5/0.5/0.0                 | 1.5          | 1167.1/805.3/685.3   | 2.5/0.6/0.0                 | 2.6          |
| 2w-I   | 988.7/602.8/532.2  | 0.8/0.2/0.2                 | 0.0          | 990.6/608.9/536.1    | 1.3/0.3/0.3                 | 0.0          |
| 2w-II  | 898.9/602.4/561.1  | 0.7/0.3/0.1                 | 2.1          | 899.3/614.6/568.6    | 1.2/1.0/0.2                 | 1.5          |
| 2w-III | 1128.4/480.0/418.6 | 2.9/0.1/0.8                 | 6.4          | 1137.1/490.4/423.5   | 3.4/0.3/0.6                 | 3.7          |
| 2w-IV  | 1136.3/482.1/408.3 | 3.0/0.2/1.1                 | 6.8          | 1147.0/490.7/419.2   | 3.4/0.2/0.2                 | 3.8          |
| 3w-I   | 835.9/412.7/401.3  | 1.0/0.5/0.1                 | 0.0          | 822.8/423.3/410.5    | 1.3/0.3/0.0                 | 0.0          |
| 3w-II  | 774.6/435.9/402.9  | 1.2/0.9/0.4                 | 1.6          | 776.7/447.1/412.3    | 1.5/0.8/0.3                 | 0.9          |
| 3w-III | 826.3/448.1/390.2  | 1.3/1.0/0.8                 | 2.0          | 828.9/462.7/399.0    | 1.8/1.0/1.1                 | 1.9          |
| 3w-IV  | 746.0/424.6/396.8  | 1.8/0.9/0.8                 | 4.5          | 751.9/439.2/407.5    | 2.0/1.2/1.2                 | 4.1          |
| 3w-V   | 913.9/387.4/314.6  | 1.7/0.5/0.1                 | 7.3          | 917.8/390.9/318.7    | 2.2/0.2/0.5                 | 5.6          |

<sup>a</sup> Equilibrium rotational constants, in MHz ; <sup>b</sup> absolute values of the components of the permanent dipole moment, in Debye ; <sup>c</sup> Relative energy, including ZPE corrections, in  $\text{kJ mol}^{-1}$ .

Fig. 1. Using the constants from quantum chemical calculations, the transitions belonging to two monohydrates, three dihydrates and three trihydrates could be assigned. Some *b*- and *c*-types transitions were measured for the monohydrates, but they were too weak to be measured for any other hydrate. Some transitions of one of the dihydrates (corresponding to the lowest energy conformer 2w-I) measured using the cavity-based spectrometer were found split into two components separated by a few kHz, showing a 3:1 intensity ratio characteristic of water tunneling motion, which results in an interchange between the bonded and non-bonded water hydrogen atoms. An example of such a line is given in Fig. S4(ESI,†). Most of the lines exhibit non resolved splittings, and in addition, they can not be observed in the chirped-pulse spectra, which means that in the analysis, we have taken into account the frequencies of the ortho component each time the splitting was resolved. The rotational constants of the water-<sup>18</sup>O isotopologues were predicted by scaling the rotational constants, using the MP2/6-311++G(d,p) geometries. The spectra of the mono- and dihydrates were directly searched for using the cavity-based spectrometer, as well as the spectra of the trihydrates with three H<sub>2</sub><sup>18</sup>O molecules. The lines were located very close to their predicted frequencies, *i.e.* within  $\pm 2$  MHz. However, the numerous spectra related to the three trihydrates with one or two H<sub>2</sub><sup>18</sup>O molecules were analysed from the broadband spectra. The measured transitions (see ESI,†) were successfully fitted using a Watson's Hamiltonian set up in the *I'* representation and reduction A, as implemented in the Pickett's suite of programs (SPFIT, SPCAT).<sup>51</sup> The inclusion of quartic centrifugal distortion were found necessary in order for all transitions to be fitted within their expected measurement accuracy. The results of the fits are given in Table 2, and those related to the isotopologues in the ESI (†).

Each spectrum could be unambiguously ascribed to its corresponding geometry by comparing the experimental and computed rotational constants, except for one dihydrate. Indeed, two very close geometries corresponding to the highest energy conformers were optimized, namely 2w-III and 2w-IV. Despite the energy ordering, comparison of experimental data with the computed ones are in favour of the highest conformer 2w-IV. The experimental second planar moment  $P_{cc}$  is  $126.4174(23) \text{ u}^2 \text{ \AA}^2$ , which agrees very well with the value  $127.59 \text{ u}^2 \text{ \AA}^2$  obtained from the computed rotational constants of 2w-IV. Using those of 2w-III, we obtained  $146.68 \text{ u}^2 \text{ \AA}^2$ , far away from the experimental one. The other two second planar moments  $P_{aa}$  and  $P_{bb}$  are also in fair agreement with the values related to 2w-IV. All hydrates have similar centrifugal distortion constants, except the monohydrate 1w-II, which has  $\Delta_J$ ,  $\Delta_{JK}$  and  $\delta_J$  one order of magnitude larger, and larger  $\Delta_K$  and  $\delta_K$ . This indicates that the water molecule is not as tightly anchored to fenchone in 1w-II as in the other hydrates.

The set of rotational constants of each hydrate (normal and isotopic species) was used to derive experimental structures by two independent methods. Both rely on the assumption that the molecular geometry is not affected by isotopic substitutions, which is generally the case for heavy atoms. The first method consists in calculating the absolute values of the coordinates of the substituted oxygen atoms by solving Kraitchman's equations,<sup>52</sup>

which make use of the slight variations of the second planar moments upon substitution. The signs of the coordinates can be inferred from those of the optimized geometries. The comparison of the substitution coordinates, collected in the ESI(†), with those given by the quantum chemical calculations confirms that the observed hydrates are correctly identified. Large substitution coordinates are expected to be reliable. For all the hydrates, this mainly concerns the coordinates along the *a* axis. In these cases, the agreement between experimental and computed coordinates is very satisfactory. For small coordinates (typically less than  $1 \text{ \AA}$ ), the agreement may be poorer, especially in the case of 2w-IV (see Table S18, ESI, †). It should be mentioned that in the case of the trihydrates, all the coordinates are in very good agreement with each other, which at first glance may be surprising since rovibrational contributions are expected to be larger in trihydrates than in monohydrates.

The second method consists in fitting internal structural parameters (bond lengths, bond angles and dihedral angles) to all available inertial moments of a given hydrate to obtain the ground state or effective  $r_0$  structure. The fit was limited to the arrangement of water molecules around fenchone. Indeed, the number of structural parameters to be fitted is much higher than the available number of rotational constants, which means that additional experimental and theoretical data have to be used. In particular, the geometry of fenchone is believed to be slightly affected by the complexation with water. The effective geometry of fenchone determined by Loru *et al.*<sup>23</sup> was then fixed in the fit. In addition, the structural parameters involving the water hydrogen atoms were taken from the computed geometry at the MP2/6-311++G(d,p) level and were also fixed in the fit. We are left with the bond lengths, bond angles and dihedral angles involving the water oxygen atoms. The results of the fits are presented in the ESI(†) and are also displayed in Fig. 2.

The energy ordering of the hydrates given by the BSSE and SAPT calculations listed in Table 3 can be viewed in parallel with their structural features. Indeed, the characteristics of the hydrogen bonds and of the van der Waals (vdW) interactions are the parameters that mostly affect the stability of the complexes. Ideally, a  $-\text{C}=\text{O}\cdots\text{H}-\text{O}$  HB should lay in the plane defined by the C=O carbon-oxygen double bond and the two oxygen lone pairs. In addition, the  $\angle(-\text{C}=\text{O}\cdots\text{O}-\text{H})$  HB angle should be close to  $120^\circ$  in order to maximise the overlap between molecular orbitals. The most significative vdW interactions take place when the  $r(\text{H}-\text{O}\cdots\text{H}-\text{C})$  distance is smaller than the sum of vdW radii of O and H, *i.e.*  $2.72 \text{ \AA}$ . They can be visualized in the NCI plots depicted in Fig. 2 as dark green surfaces. The results of the SAPT calculations are presented in Table 3, along with the complexation energies from BSSE calculations at the MP2/6-311++G(d,p) level. The energy ordering of the monohydrates can be easily rationalized considering the HB and the vdW interactions. Indeed, the difference in energy between 1w-I and 1w-II is mostly due to the electrostatic contribution to the total energy, with a significant difference close to  $8 \text{ kJ mol}^{-1}$ , correlated with the strength of the  $\text{O}-\text{H}\cdots\text{O}=\text{C}$  hydrogen bond, and hence to the  $r(\text{H}\cdots\text{O})$  bond lengths, calculated to be  $1.940(7) \text{ \AA}$  in 1w-I and  $1.965(2) \text{ \AA}$  in 1w-II from the  $r_0$  coordinates given by the fits. In addition, in 1w-I

**Table 2** Experimental ground state rotational and centrifugal distortion constants of the hydrates of fenchone

| Parameter <sup>a,b</sup>    | Monohydrates   |                |                | Dihydrates    |               |  |
|-----------------------------|----------------|----------------|----------------|---------------|---------------|--|
|                             | 1w-I           | 1w-II          | 2w-I           | 2w-II         | 2w-IV         |  |
| $A$ / MHz                   | 1288.79191(18) | 1150.18315(30) | 983.2739(21)   | 882.5076(36)  | 1153.237(12)  |  |
| $B$ / MHz                   | 739.998659(45) | 793.033620(63) | 591.32083(20)  | 591.87733(21) | 479.53721(25) |  |
| $C$ / MHz                   | 608.776708(32) | 672.035636(34) | 523.53413(14)  | 549.00620(16) | 407.80026(27) |  |
| $\Delta_J$ / kHz            | 0.05199(20)    | 0.54348(34)    | 0.05632(49)    | 0.07147(97)   | 0.0437(15)    |  |
| $\Delta_{JK}$ / kHz         | 0.25089(93)    | -0.7295(25)    | 0.2722(75)     | 0.320(14)     | 0.284(10)     |  |
| $\Delta_K$ / kHz            | -0.1799(86)    | 0.632(12)      | -              | -             | -             |  |
| $\delta_J$ / kHz            | 0.00628(10)    | -0.03948(18)   | 0.00546(44)    | 0.00672(72)   | -             |  |
| $\delta_K$ / kHz            | 0.0444(25)     | 0.0961(23)     | -              | -             | -             |  |
| $\sigma_{\text{fit}}$ / kHz | 1.99           | 8.01           | 3.89           | 4.09          | 4.51          |  |
| $N_{\text{lines}}$          | 91             | 74             | 60             | 40            | 51            |  |
|                             | Trihydrates    |                |                |               |               |  |
|                             | 3w-I           | 3w-II          | 3w-III         |               |               |  |
| $A$ / MHz                   | 825.2745(94)   | 756.3620(34)   | 820.5228(14)   |               |               |  |
| $B$ / MHz                   | 406.893833(93) | 431.82218(20)  | 449.00647(12)  |               |               |  |
| $C$ / MHz                   | 396.499381(82) | 396.89694(11)  | 393.456862(81) |               |               |  |
| $\Delta_J$ / kHz            | 0.04150(21)    | 0.05504(57)    | 0.05590(45)    |               |               |  |
| $\Delta_{JK}$ / kHz         | 0.0208(35)     | 0.1442(65)     | -              |               |               |  |
| $\Delta_K$ / kHz            | -              | -              | -              |               |               |  |
| $\delta_J$ / kHz            | 0.00397(29)    | 0.01016(52)    | 0.01313(40)    |               |               |  |
| $\delta_K$ / kHz            | -              | -              | -              |               |               |  |
| $\sigma_{\text{fit}}$ / kHz | 2.99           | 1.55           | 1.42           |               |               |  |
| $N_{\text{lines}}$          | 45             | 37             | 37             |               |               |  |

<sup>a</sup>  $A$ ,  $B$ ,  $C$  are the ground state rotational constants;  $\Delta_J$  to  $\delta_K$  are the five quartic centrifugal distortion constants;  $\sigma_{\text{fit}}$  is the standard deviation of the fit and  $N_{\text{lines}}$  are the number of transitions included in the fit; <sup>b</sup> Numbers in parentheses are standard errors ( $1\sigma$ , 67% confidence level) in units of the last digit.

**Table 3** Decomposition of the interaction energy between fenchone and water as calculated at the SAPT2+ / aug-cc-PVDZ level of theory, and BSSE corrected interaction energies at the MP2/6-311++G(d,p) level. All values in  $\text{kJ mol}^{-1}$ .

|        | $E_{\text{elec}}$ | $E_{\text{exch}}$ | $E_{\text{ind}}$ | $E_{\text{disp}}$ | $E_{\text{SAPT2+}}$ | $E_{\text{BSSE}}$ |
|--------|-------------------|-------------------|------------------|-------------------|---------------------|-------------------|
| 1w-I   | -46.50            | 52.78             | -16.37           | -19.91            | -27.27              | -29.99            |
| 1w-II  | -38.56            | 44.39             | -13.88           | -18.61            | -24.43              | -26.67            |
| 2w-I   | -55.76            | 64.73             | -22.58           | -31.03            | -44.64              | -36.53            |
| 2w-II  | -58.52            | 68.90             | -24.50           | -29.32            | -43.44              | -35.90            |
| 2w-III | -56.27            | 62.07             | -22.74           | -23.94            | -40.89              | -33.05            |
| 2w-IV  | -55.80            | 62.43             | -22.76           | -23.99            | -40.11              | -33.08            |
| 3w-I   | -69.62            | 80.24             | -29.71           | -35.83            | -54.92              | -44.69            |
| 3w-II  | -71.27            | 84.01             | -30.99           | -35.29            | -53.54              | -43.64            |
| 3w-III | -66.56            | 79.79             | -29.94           | -36.39            | -53.09              | -42.22            |
| 3w-IV  | -64.19            | 73.63             | -28.60           | -30.99            | -50.16              | -41.49            |
| 3w-V   | -66.25            | 78.21             | -28.74           | -34.39            | -51.17              | -40.44            |

the water molecule lays in the plane of the  $-\text{C}=\text{O}$  bond, while in 1w-II the  $\tau_{\text{HB}}(-\text{C}-\text{C}=\text{O}\cdots\text{H})$  dihedral angle is  $-44.60(20)^\circ$ , due to the presence of a methyl group, which strongly disadvantages the establishment of the HB.

The interpretation of the results concerning the dihydrates is not straightforward. In 2w-I and 2w-II, the HB angle is respectively  $125.4(15)^\circ$  and  $124.09(55)^\circ$ . The deviation from the ideal value of  $120^\circ$  is then very small and can not explain the differences of the electrostatic contributions to the energy. We have to refer to the  $\tau_{\text{HB}}(-\text{C}-\text{C}=\text{O}\cdots\text{H})$  dihedral angle to account for the differences. Indeed, the value of  $\tau_{\text{HB}} = -54.0(2)^\circ$  in 2w-I strongly disadvantaged the establishment of the HB, which may explain why the electrostatic contribution in 2w-I is the smallest among

the four dihydrates. It is the highest in 2w-II and it can not be only due to the HB, but also to a vdW interaction occurring at a distance of  $2.427(10)\text{ \AA}$  which may have an electrostatic character. The contribution of dispersion to the total energy is much higher in 2w-I and 2w-II than in 2w-IV because in this conformer, there is only one interaction at a short distance between the last oxygen atom and an hydrogen atom of one of the methyl group (Fig. 2e). In 2w-I, there are three such interactions (Fig. 2c), and two in 2w-II, with one occurring at a rather short distance of  $2.427(10)\text{ \AA}$ . The first oxygen atom of the water dimer does not interact with hydrogen atoms of fenchone in any of the dihydrates, at least at distances lower than  $2.7\text{ \AA}$ . These differences qualitatively appear when comparing the NCI plots shown in Fig. 2c and Figs. 2d and 2e. Indeed, in 2w-I, there is a wide green isosurface related to numerous vdW interactions between the two water molecules and fenchone, while in 2w-II and 2w-IV, they are more directional. The other two dihydrates 2w-III and 2w-IV are separated by  $0.78\text{ kJ mol}^{-1}$  according to the SAPT calculations, but are calculated at the same energy according to the BSSE calculation.

In camphor, no dihydrates exhibiting the same geometries as our 2w-I and 2w-II conformers (*i.e.* with the water dimer directed towards the methyl group) could be assigned,<sup>17</sup> even though this part of the molecule is the same in camphor and fenchone.

The isolated water trimer adopts a cyclic H-bonded structure which maximizes the cooperativity between HBs. It has been shown that in the trihydrates of aromatic hydrocarbons, the cyclic structure is retained. The water trimer sits above the aromatic rings, in complexes with benzene<sup>53</sup> and acenaphtene.<sup>54,55</sup> How-

ever, in terpenoids, water has the opportunity to form a strong HB with the  $-C=O$  moiety, as documented in studies involving carboxylic acids,<sup>56,57</sup> aldehydes,<sup>20</sup> and ketones.<sup>17,18</sup> The results on fenchone hydrates confirm this trend. For the first time, three trihydrates were experimentally characterized, which gives us the opportunity to compare their geometry. One end of the chain of three molecules of water is linked to fenchone by a HB that has a length of 1.837(22) Å in 3w-I, of 1.769(38) Å in 3w-II and of 1.887(20) Å in 3w-III. They are shorter than in the monohydrates (1.940(7) Å in 1w-I) and dihydrates (1.904(20) Å in 2w-I). The internal HB of the water dimer attached to fenchone is also slightly shorter (1.913(17) Å in 2w-I) than in the isolated water dimer (1.949 Å calculated at the MP2/6-311++G(d,p) level). For instance, in 3w-I, we have  $r(H_{w_3}O_1) = 1.868(15)$  Å and  $r(H_{w_5}O_2) = 1.826(12)$  Å. This is a consequence of the cooperativity between HB that confers a higher stability to the trihydrates.<sup>58,59</sup> The length of the  $-C=O\cdots O-H$  HB is correlated to the electrostatic contribution to the complexation energy and can explain the difference of 1.65 kJ mol<sup>-1</sup> between 3w-I and 3w-II, and of 4.71 kJ mol<sup>-1</sup> between 3w-II and 3w-III. The latter difference is also due to a tilt in the arrangement of the water chain with a dihedral angle  $\tau(O_fO_1O_2O_3) = 12.82(78)^\circ$  that reduces the effect of cooperativity. Dispersion is almost the same in the three trihydrates since the last oxygen atom interacts with two alkyl hydrogen atoms of fenchone. Nevertheless, as in 2w-I, a continuous green isosurface is observed in 3w-I (Fig. 2f), and to a lesser extent in 3w-III (Fig. 2h), but not in 3w-II (Fig. 2g). It should be noticed that the last oxygen atom of the chain interacts with the same alkyl protons of fenchone in 3w-I and 3w-III. But in this last conformer, the first HB ( $O-H\cdots O=C$ ) is directed towards the two methyl groups (*i.e.* in the opposite direction relatively to 1w-I), and the chain of water molecules then turns towards the methyl group to finally interact with it. The conformer 3w-II is the analogue of the trihydrate found for camphor.<sup>17</sup>

The relative abundances of the hydrates in the jet were estimated by the ratio of the intensities of common selected  $a$ -type lines present in the chirped-pulse spectrum over the square of the corresponding MP2 dipole moment component. The estimated values of the relative abundances are 1w-I:1w-II = 3.2 : 1.0, 2w-1:2w-II:2w-III = 59:46:1, and 3w-I:3w-II:3w-III = 2.7 : 1.3 : 1.0. These abundances are in qualitative agreement with the relative energies of the complexes and the values of the interaction energies in Table 3. There is a very large difference in relative abundance for the 2w-IV complex. The rotational transitions of 2w-IV lie at very different frequencies than those of 2w-I and 2w-II due to its different rotational constants, and its dipole moment along the  $a$  inertial axis is much larger than those of 2w-I and 2w-II. This may skew the estimated value of the relative abundance of 2w-IV, but although it must be taken with caution, it is evident that 2w-IV is much less abundant than the other 2w complexes. In the dihydrates and trihydrates, the lowest energy conformers are those where the chain of water avoids the steric hindrance of the methyl groups. There is a notable change in the configurational preferences in going from the monohydrates to the di- and trihydrates. In the monohydrates, the most abundant complex is the one that maximises electrostatic interactions by optimising

the  $O-H\cdots O$  hydrogen bond, the overlap between the carbonyl oxygen lone pair and the hydrogen atom of water. However, in the 2w and 3w complexes this preference is reversed to favour a less optimal  $O-H\cdots O$  bonding to fenchone that is compensated with a higher number of secondary interactions between water and fenchone and an arrangement that enhances hydrogen bonding within the water molecules.

The observed configurational preferences of the hydrates of fenchone show how subtle changes in structure completely change the relative arrangements of the water subunits. Camphor, a structural isomer of fenchone, has a methyl substituted carbon in alpha with respect to the carbonyl group like fenchone, but the dimethyl substituted carbon is in a different position and does not directly affect primary  $O-H\cdots O$  bonding by water. Hence water preferentially binds to camphor through the lone pair of the carbonyl oxygen away from the methyl substituted alpha carbon, and this preference is maintained in the dihydrate and trihydrate observed. In fenchone, the presence of two additional methyl groups in alpha modifies the possible interactions and results in a more intricate configurational picture. This has also been observed in the complexes of fenchone with ethanol, phenol and benzene,<sup>24,25</sup> where the preferred binding site changed as dispersion interactions became more prominent.

## 4 Conclusions

In this study, we have experimentally characterized two monohydrates, three dihydrates and three trihydrates of fenchone using both chirped-pulse and cavity-based Fourier transform microwave spectrometers. The molecular cohesion is due to a hydrogen bond between the carbonyl moiety of fenchone and water, but a complex network of van der Waals interactions of water oxygen atoms with hydrogen alkyl groups complete the anchor of water molecules to fenchone. In addition, they govern the energy ordering of the hydrates, as shown by SAPT calculations. Considering that the hydrates may be formed from preexisting water clusters (although this point has never been clearly established), and that clusters of up to ten water molecules were characterized in supersonic jets,<sup>60-62</sup> it should be interesting to extend the investigations to even more solvated molecules, and learn how the balance of forces changes. Could a chain of four, five, six water molecules be attached to a molecule like fenchone ?

## 5 Conclusions

In this study, we have experimentally characterized two monohydrates, three dihydrates and three trihydrates of fenchone using both chirped-pulse and cavity-based Fourier transform microwave spectrometers. The molecular cohesion is due to a hydrogen bond between the carbonyl moiety of fenchone and water, but a complex network of van der Waals interactions of water oxygen atoms with hydrogen alkyl groups complete the anchor of water molecules to fenchone. In addition, they govern the energy ordering of the hydrates, as shown by SAPT calculations. Considering that the hydrates may be formed from preexisting water clusters (although this point has never been clearly established), and that clusters of up to ten water molecules were characterized in supersonic jets,<sup>60-62</sup> it should be interesting to extend the in-



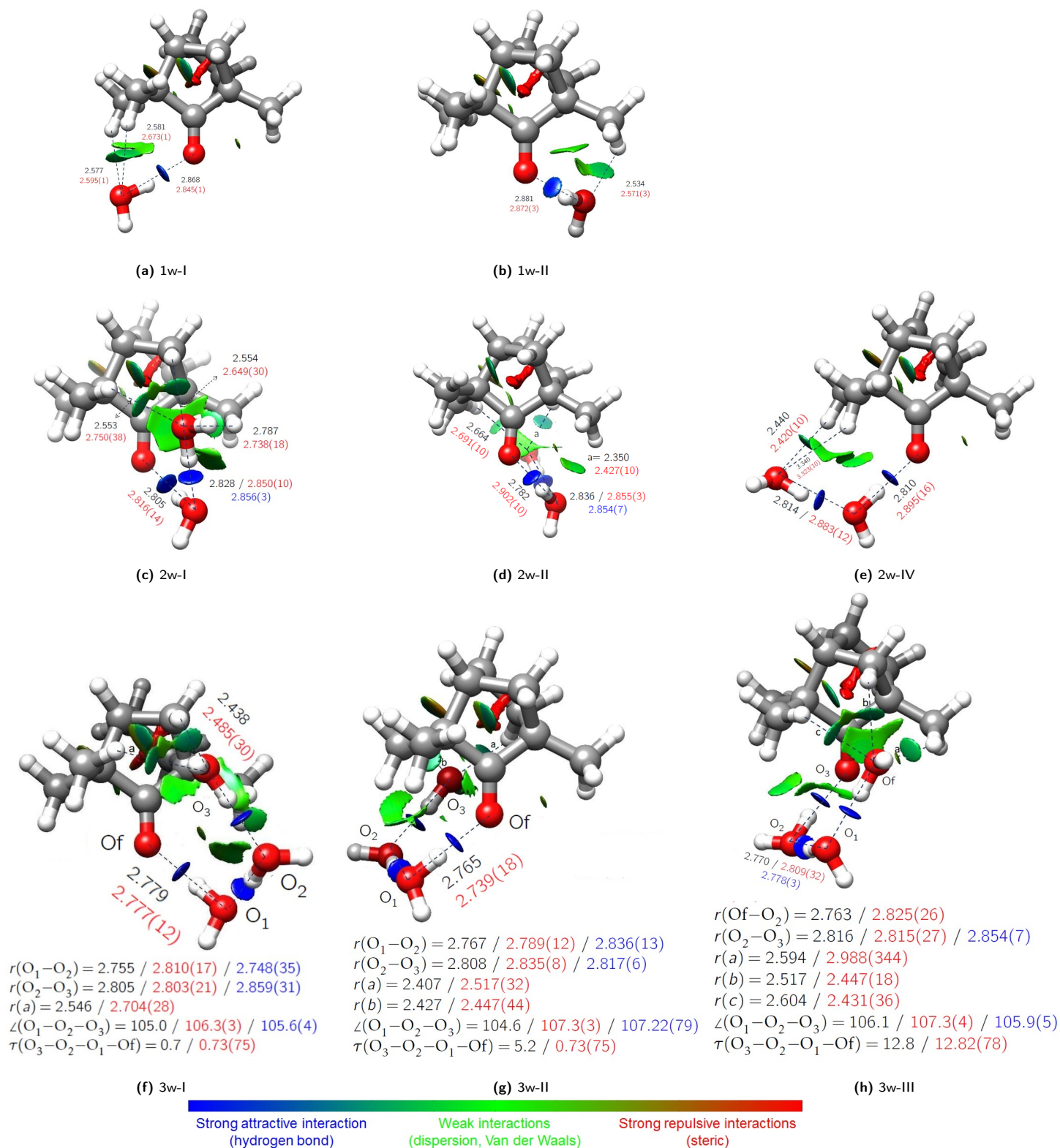


**Fig. 2** NCI plots corresponding to  $s = 0.5$  showing the vdW interactions in the hydrates of fenone. Values of  $\text{sign}(\lambda_2)\rho$  are comprised within  $-0.05$  au and  $+0.05$  au. The structural parameters (bond lengths in Å, bond and dihedral angles in °) written in black, red and blue respectively correspond to the MP2/6-311++G(d,p), the  $r_0$  and the substitution parameters.

vestigations to even more solvated molecules, and learn how the balance of forces changes.. Could a chain of four, five, six water molecules be attached to a molecule like fenone ?

## Conflicts of interest

There are no conflicts to declare.



## Acknowledgements

The present work was funded by the French ANR Labex CaPPA through the PIA under contract ANR-11-LABX-0005-01, by the Regional Council Hauts de France, the European Funds for Regional Economic Development (FEDER), by the French Ministère de l'Enseignement Supérieur et de la Recherche. It is a contribution to the CPER research Project CLIMIBIO. It was also funded by the UE FP7 (Marie Curie grant PCIG12-GA-2012-334525), EPSRC (EP/N509498/1) and King's College London.

## Notes and references

- 1 M. Shrivastava, M. Andrae, P. Artaxo, H. Barbosa, L. Berg, J. Brito, J. Ching, R. Easter, J. Fan, J. Fast, Z. Feng, J. Fuentes, M. Glasius, A. Goldstein, E. Alves, H. Gomes, D. Gu, A. Guenther, S. Jathar, S. Kim, Y. Liu, S. Lou, S. Martin, V. McNeill, A. Medeiros, S. de Sá, J. Shilling, S. Springston, R. Souza, J. Thornton, G. Isaacman-VanWertz, L. Yee, R. Ynoue, R. Zaveri, A. Zelenyuk and C. Zhao, *Nat. Commun.*, 2019, **10**, 1046.
- 2 G. Churkina, F. Kuik, B. Bonn, A. Lauer, R. Grote, K. Tomiak and T. M. Butler, *Environ. Sci. Technol.*, 2017, **51**, 6120–6130.
- 3 M. Hallquist, J. Wenger, U. Baltensperger, Y. Rudich, D. Simpson, M. Claeys, J. Dommen, N. Donahue, C. George, A. Goldstein, J. Hamilton, H. Herrmann, T. Hoffmann, Y. Iinuma, M. Jang, M. Jenkin, J. Jimenez, A. Kiendler-Scharr, W. Maenhaut, G. McFiggans, T. Mentel, A. Monod, A. Prévôt, J. Seinfeld, J. Surratt, R. Szmigielski and J. Wildt, *Atmos. Chem. Phys.*, 2009, **9**, 5155–5236.
- 4 J. Jimenez, M. Canagaratna, N. Donahue, A. Prevot, Q. Zhang, J. Kroll, P. DeCarlo, J. Allan, H. Coe, N. Ng, A. Aiken, K. Docherty, I. Ulbrich, A. Grieshop, A. Robinson, J. Duplissy, J. Smith, K. Wilson, V. Lanz, C. Hueglin, Y. Sun, J. Tian, A. Laaksonen, T. Raatikainen, J. Rautiainen, P. Vaattovaara, M. Ehn, M. Kulmala, J. Tomlinson, D. Collins, M. Cubison, E. Dunlea, J. Huffman, T. Onasch, M. Alfarra, P. Williams, K. Bower, Y. Kondo, J. Schneider, F. Drewnick, S. Borrmann, S. Weimer, K. Demerjian, D. Salcedo, L. Cottrell, R. Griffin, A. Takami, T. Miyoshi, S. Hatakeyama, A. Shimono, J. Sun, Y. Zhang, K. Dzepina, J. Kimmel, D. Sueper, J. Jayne, S. Herndon, A. Trimborn, L. Williams, E. Wood, A. Middlebrook, C. Kolb, U. Baltensperger and D. Worsnop, *Science*, 2009, **326**, 1525–1529.
- 5 R. Zhang, *Science*, 2010, **328**, 1366–1367.
- 6 P. Ziemann and R. Atkinson, *Chem. Soc. Rev.*, 2012, **41**, 6582–6605.
- 7 B. Bonn, G. Schuster and G. Moortgat, *J. Phys. Chem. A*, 2002, **106**, 2869–2881.
- 8 V. Vaida, *J. Chem. Phys.*, 2011, **135**, 020901.
- 9 T. Chen, B. Chu, Q. Ma, P. Zhang, J. Liu and H. He, *Sci. Total Environ.*, 2021, **773**, 145015.
- 10 Y. Gong and Z. Chen, *Atmos. Chem. Phys.*, 2021, **21**, 813–829.
- 11 R. Zhao, Q. Zhang, X. Xu, W. Zhao, H. Yu, W. Wang, Y. Zhang and W. Zhang, *Atmos. Pollut. Res.*, 2021, **12**, 205–213.
- 12 R. Sure, M. el Mahdali, A. Plajer and P. Deglmann, *J. Comput. Aided Mol. Des.*, 2021, **35**, 473–492.
- 13 W. Jesus, F. Prudente, J. Marques and F. Pereira, *Phys. Chem. Chem. Phys.*, 2021, **23**, 1738–1749.
- 14 G. Simm, P. Türtcher and M. Reiher, *J. Comput. Chem.*, 2020, **41**, 1144–1155.
- 15 M. Steiner, T. Holzknacht, M. Schauperl and M. Podewitz, *Molecules*, 2021, **26**, 1793.
- 16 A. Legon, *Annu. Rev. Phys. Chem.*, 1983, **34**, 275–300.
- 17 C. Pérez, A. Krin, A. Steber, J. López, Z. Kisiel and M. Schnell, *J. Phys. Chem. Lett.*, 2016, **7**, 154–160.
- 18 M. Chrayteh, A. Savoia, T. Huet and P. Dréan, *Phys. Chem. Chem. Phys.*, 2020, **22**, 5855–5864.
- 19 M. Chrayteh, T. Huet and P. Dréan, *J. Phys. Chem. A*, 2020, **124**, 6511–6520.
- 20 M. Chrayteh, T. Huet and P. Dréan, *J. Chem. Phys.*, 2020, **153**, 104304.
- 21 S. Blanco, J. C. López and A. Maris, *Phys. Chem. Chem. Phys.*, 2020, **22**, 5729–5734.
- 22 S. I. Murugachandran, J. Tang, I. Peña, D. Loru and M. E. Sanz, *J. Phys. Chem. Lett.*, 2021, **12**, 1081–1086.
- 23 D. Loru, M. A. Bermúdez and M. E. Sanz, *J. Chem. Phys.*, 2016, **145**, 1627–1638.
- 24 D. Loru, I. Peña and M. Sanz, *Phys. Chem. Chem. Phys.*, 2019, **21**, 2938–2945.
- 25 E. Burevschi, E. R. Alonso and M. E. Sanz, *Chem. Eur. J.*, 2020, **26**, 11327–11333.
- 26 M. J. Frisch, G. W. Trucks, H. B. Schlegel, G. E. Scuseria, M. A. Robb, J. R. Cheeseman, G. Scalmani, V. Barone, G. A. Petersson, H. Nakatsuji, X. Li, M. Caricato, A. V. Marenich, J. Bloino, B. G. Janesko, R. Gomperts, B. Mennucci, H. P. Hratchian, J. V. Ortiz, A. F. Izmaylov, J. L. Sonnenberg, D. Williams-Young, F. Ding, F. Lipparini, F. Egidi, J. Goings, B. Peng, A. Petrone, T. Henderson, D. Ranasinghe, V. G. Zakrzewski, J. Gao, N. Rega, G. Zheng, W. Liang, M. Hada, M. Ehara, K. Toyota, R. Fukuda, J. Hasegawa, M. Ishida, T. Nakajima, Y. Honda, O. Kitao, H. Nakai, T. Vreven, K. Throssell, J. A. Montgomery, Jr., J. E. Peralta, F. Ogliaro, M. J. Bearpark, J. J. Heyd, E. N. Brothers, K. N. Kudin, V. N. Staroverov, T. A. Keith, R. Kobayashi, J. Normand, K. Raghavachari, A. P. Rendell, J. C. Burant, S. S. Iyengar, J. Tomasi, M. Cossi, J. M. Millam, M. Klene, C. Adamo, R. Cammi, J. W. Ochterski, R. L. Martin, K. Morokuma, O. Farkas, J. B. Foresman and D. J. Fox, *Gaussian 16 Revision B.01*, 2016, Gaussian Inc. Wallingford CT.
- 27 P. Pracht, F. Bohle and S. Grimme, *Phys. Chem. Chem. Phys.*, 2020, **22**, 7169–7192.
- 28 S. Grimme, *J. Chem. Theory Comput.*, 2019, **15**, 2847–2862.
- 29 P. Stephens, F. Devlin, C. Chabalowski and M. Frisch, *J. Phys. Chem.*, 1994, **98**, 11623–11627.
- 30 S. Grimme, *J. Comput. Chem.*, 2004, **25**, 1463–1473.
- 31 S. Grimme, J. Antony, S. Ehrlich and H. Krieg, *J. Chem. Phys.*, 2010, **132**, 154104.
- 32 S. Grimme, *Wiley Interdiscip. Rev.: Comput. Mol. Sci.*, 2011, **1**, 211–228.

- 33 A. Becke, *Phys. Rev. A*, 1988, **38**, 3098–3100.
- 34 A. Becke, *J. Chem. Phys.*, 1993, **98**, 5648–5652.
- 35 E. Johnson and A. Becke, *J. Chem. Phys.*, 2005, **123**, 024101.
- 36 E. Johnson and A. Becke, *J. Chem. Phys.*, 2006, **124**, 174104.
- 37 F. Weigend and R. Ahlrichs, *Phys. Chem. Chem. Phys.*, 2005, **7**, 3297–3305.
- 38 C. Møller and M. S. Plesset, *Phys. Rev.*, 1934, **46**, 618–622.
- 39 W. Hehre, K. Ditchfield and J. Pople, *J. Chem. Phys.*, 1972, **56**, 2257–2261.
- 40 R. Krishnan, J. Binkley, R. Seeger and J. Pople, *J. Chem. Phys.*, 1980, **72**, 650–654.
- 41 M. Frisch, J. Pople and J. Binkley, *J. Chem. Phys.*, 1984, **80**, 3265–3269.
- 42 S. Boys and F. Bernardi, *Mol. Phys.*, 1970, **19**, 553–566.
- 43 B. Jeziorski, R. Moszynski and K. Szalewicz, *Chem. rev.*, 1994, **94**, 1887–1930.
- 44 T. Parker, L. Burns, R. Parrish, A. Ryno and C. Sherrill, *J. Chem. Phys.*, 2014, **140**, 094106.
- 45 E. Johnson, S. Keinan, P. Mori-Sánchez, J. Contreras-García, A. Cohen and W. Yang, *J. Am. Chem. Soc.*, 2010, **132**, 6498–6506.
- 46 R. Laplaza, F. Peccati, R. A. Boto, C. Quan, A. Carbone, J.-P. Piquemal, Y. Maday and J. Contreras-García, *Wiley Interdiscip. Rev.: Comput. Mol. Sci.*, 2020, e1497.
- 47 W. Humphrey, A. Dalke and K. Schulten, *J. Mol. Graph.*, 1996, **14**, 33–38.
- 48 S. Kassi, D. Petitprez and G. Wlodarczak, *J. Mol. Spectrosc.*, 2004, **228**, 293–297.
- 49 D. Loru, I. Peña and M. E. Sanz, *J. Mol. Spectrosc.*, 2017, **335**, 93 – 101.
- 50 C. Bannwarth, S. Ehlert and S. Grimme, *J. Chem. Theory Comput.*, 2019, **15**, 1652–1671.
- 51 H. M. Pickett, *J. Mol. Spectrosc.*, 1991, **148**, 371 – 377.
- 52 J. Kraitchman, *Am. J. Phys.*, 1953, **21**, 17–24.
- 53 R. N. Pribble and T. S. Zwier, *Faraday Discuss.*, 1994, **97**, 229–241.
- 54 A. Steber, C. Pérez, B. Temelso, G. Shields, A. Rijs, B. Pate, Z. Kisiel and M. Schnell, *J. Phys. Chem. Lett.*, 2017, 5744–5750.
- 55 A. Lemmens, S. Gruet, A. Steber, J. Antony, S. Grimme, M. Schnell and A. Rijs, *Phys. Chem. Chem. Phys.*, 2019, **21**, 3414–3422.
- 56 O. Bin, T. Starkey and B. J. Howard, *J. Phys. Chem. A*, 2007, **111**, 6165–6175.
- 57 B. Ouyang, T. G. Starkey and B. J. Howard, *J. Phys. Chem. A*, 2007, **111**, 6165–6175.
- 58 S. Scheiner, *Theor. Comput. Chem.*, 1999, **6**, 571–591.
- 59 K. Liu, J. Cruzan and R. Saykally, *Science*, 1996, **271**, 929–933.
- 60 C. Pérez, M. Muckle, D. Zaleski, N. Seifert, B. Temelso, G. Shields, Z. Kisiel and B. Pate, *Science*, 2012, **336**, 897–901.
- 61 C. Pérez, S. Lobsiger, N. Seifert, D. Zaleski, B. Temelso, G. Shields, Z. Kisiel and B. Pate, *Chem. Phys. Lett.*, 2013, **571**, 1–15.
- 62 C. Pérez, D. Zaleski, N. Seifert, B. Temelso, G. Shields, Z. Kisiel and B. Pate, *Angew. Chem., Int. Ed.*, 2014, **53**, 14368–14372.